J. Fluid Mech. (1973), *vol.* 59, *part* 2, *pp.* 239–256
Printed in Great Britain

The damping of surface gravity waves in a bounded liquid

By C. C. MEI AND L. F. LIU
Department of Civil Engineering, Massachusetts Institute of Technology

(Received 24 July 1972 and in revised form 15 January 1973)

In deducing the viscous damping rate in surface waves confined by side walls, Ursell found in an example that two different calculations, one by energy dissipation within and the other by pressure working on the edge of the side-wall boundary layers, gave different answers. This discrepancy occurs in other examples also and is resolved here by examining the energy transfer in the neighbourhood of the free-surface meniscus. With due care near the meniscus a boundary-layer–Poincaré method is employed to give an alternative derivation for the rate of attenuation and to obtain in addition the frequency (or wave-number) shift due to viscosity. Surface tension is not considered.

1. Introduction

The calculation of surface-wave damping in a slightly viscous liquid (with viscosity ν) confined by solid walls is a well-known problem. In the most common approach (Hunt 1952; Ursell 1952; Case & Parkinson 1957; Keulegan 1959; Miles 1967, etc.), it is assumed that for infinitesimal waves of frequency σ the motion is essentially irrotational except near the boundaries, where viscous boundary layers of thickness of order $(\nu/\sigma)^{\frac{1}{2}}$ are formed. Energy dissipation takes place in (*a*) the boundary layers near the solid walls, (*b*) the boundary layer near the free surface and (*c*) the essentially inviscid core. If the free surface is uncontaminated, these contributions are respectively proportional to $\nu^{\frac{1}{2}}$, $\nu^{\frac{3}{2}}$ and ν (see, for example, Ursell 1952). Thus the wall boundary layers are the most significant. As the net rate of dissipation must be balanced by the slow rate of decay of wave energy, the damping rate is found.

In checking his theory on edge waves with laboratory experiments Ursell (1952) calculated the wave damping rate in two ways: one by adding up the dissipation rates in the boundary layers adjacent to the side walls and the bottom, and the other by deducing the rate of pressure working from the essentially inviscid interior to the wall boundary layer. The two methods gave different results. Ursell argued that since the first one must be correct, there should be a mathematical singularity at the free-surface meniscus. Similar calculations by us for standing waves in rectangular and circular basins of constant depth and for progressive waves in a uniform channel showed the same discrepancy, suggesting that the 'singularity' is not limited to a few circumstances but is of quite general nature. The first purpose of this paper is to clarify the physical origin of this singularity and to resolve the discrepancy. After the derivation of certain pertinent results including the damping rates by a perturbation analysis, the physical nature of this singularity is examined by a detailed discussion of energy transfer. It is found that the free-surface meniscus is a vital gateway by which energy leaks through from the waves to the side-wall boundary layer.

A second purpose of this paper is to derive more completely the first-order effect of small viscosity on the dispersion relation. More specifically, if the wavenumber is kept real, the frequency changes by a small amount which is *complex* with the imaginary part corresponding to the attenuation rate and the real part to the frequency shift. In progressive waves one usually keeps the frequency real, then it is the wavenumber which suffers a slight *complex* change.

In earlier theories little attention is given to the real frequency (or wavenumber) shift. Consider, however, weakly nonlinear waves in real fluids: the evolution of such waves involves time scales much longer than a wave period and often a term of second order in wave slope, $O(ka)^2$, must be added in the dispersion relation. On the other hand, in certain cases the frequency shift due to the bottom boundary layer is known to be of $O(k\delta)$ (Hunt 1964; Johns 1968), where $\delta = (\nu/\sigma)^{\frac{1}{2}}$ is the Stokes boundary-layer thickness. In laboratory experiments the effects of viscosity and nonlinearity are often comparable (Chu & Mei 1971), i.e.

$$O(k\delta) = O(ka)^2.$$

Consider next the linearized theory of forced oscillations: it is known that damping shifts the resonant peaks slightly away from the inviscid natural frequency. In the neighbourhood of sharp peaks on an amplitude–frequency response curve the shift in real frequency may be of equal importance for predicting correctly the response amplitude. It is therefore desirable to work out the whole complex frequency (or wavenumber) change due to viscosity.

To the lowest order of approximation it is reasonable to expect that the first corrections for small viscosity and weak nonlinearity are uncoupled, hence to examine the former we formulate the problem here on the basis of a linearized viscous theory just as in all existing theories on damping rates. The conventional energy dissipation argument, however, gives only the damping rate and not the frequency shift. For two-dimensional problems with side walls two methods can be employed. The first is to solve the eigenvalue problem with the full linearized Navier–Stokes equations and boundary conditions without the assumption of small viscosity. This approach is extremely tedious (Hunt 1964) and has not been applied to three-dimensional problems. The second is to use the boundary-layer–Poincaré technique,† whose efficacy has been demonstrated by Greenspan (1968, chap. 2) for contained rotating fluid without a free surface and by Johns (1968) and Dore (1968) for two-dimensional free-surface problems without side walls. The boundary-layer–Poincaré method is employed here for small amplitude waves in a basin or a channel with a free surface. The meniscus 'singularity' alluded to earlier requires that the perturbation method be executed with greater care than in the cited cases, where this method was applied but

† An equivalent argument was first used by Longuet-Higgins (1951) for progressive waves without side walls.

where the free surface and the side walls were not present jointly. Indeed serious errors were committed by us in an earlier draft. The examples given here indicate also that application of this technique to similar problems, e.g. interfacial waves in a container, must be treated with equal care.

2. Analysis

2.1. *Formulation*

We first summarize the *linearized* governing equations and boundary conditions for a small amplitude wave in a liquid bounded by the solid surface S and the free surface F (see, for example, Wehausen & Laitone 1960, p. 640). Cartesian co-ordinates (x', y', z') are employed and fixed on the mean free surface $z' = 0$, where z' is positive upward. The following dimensionless variables are adopted here using the inverse k^{-1} of a characteristic wavenumber as the length scale and the inviscid wave amplitude a_0 as the scale of motion:

$$\left.\begin{aligned} (x,y,z) &= k(x',y',z'), & t &= (gk)^{\frac{1}{2}}t', \\ (u,v,w) &= (u',v',w')/a_0(gk)^{\frac{1}{2}}, & \eta &= \eta'/a_0, \end{aligned}\right\} \tag{2.1}$$

where all variables with primes represent physical quantities and $z' = \eta'$ is the free-surface elevation. As is well known the linearized Navier–Stokes equations permit the velocity to be split into a potential part $\nabla\phi$ and a rotational part $\mathbf{U}$, namely

$$\mathbf{u} = \nabla\phi + \mathbf{U}, \quad \phi = \phi'[k/a_0(gk)^{\frac{1}{2}}]. \tag{2.2}$$

The total pressure is given by

$$p' = p'_d - \rho g z' = -\rho\phi'_t - \rho g z', \quad p'_d = (\rho g a_0)p_d, \tag{2.3}$$

where p'_d is the dynamic pressure. The dimensionless equations are then

$$\nabla^2\phi = 0, \tag{2.4}$$

$$\partial\mathbf{U}/\partial t = \epsilon^2\nabla^2\mathbf{U}, \tag{2.5}$$

and

$$\nabla\,.\,\mathbf{U} = 0. \tag{2.6}$$

At the solid boundary all components of velocity must vanish:

$$\nabla\phi + \mathbf{U} = 0 \quad \text{on} \quad S. \tag{2.7a}$$

Assuming no surface tension and external stresses, the normal stress and tangential stresses must vanish at the free surface:

$$\partial\phi/\partial t + \eta + 2\epsilon^2\,\partial w/\partial z = 0 \quad \text{on} \quad z = 0, \tag{2.7b}$$

$$\epsilon^2\left(\frac{\partial u}{\partial z} + \frac{\partial w}{\partial x}\right) = \epsilon^2\left(\frac{\partial v}{\partial z} + \frac{\partial w}{\partial y}\right) = 0 \quad \text{on} \quad z = 0. \tag{2.7c}$$

The linearized kinematic surface condition reads

$$\partial\eta/\partial t = w \quad \text{on} \quad z = 0. \tag{2.7d}$$

The parameter

$$\epsilon = k\nu^{\frac{1}{2}}(gk)^{-\frac{1}{4}} \ll 1 \tag{2.8}$$

is a dimensionless measure of the thickness of the oscillatory boundary layer and ϵ^{-2} may be regarded as the Reynolds number.

The condition (2.7*b*) on the normal stress and the kinematic condition (2.7*d*) may be combined to give

$$\frac{\partial^2\phi}{\partial t^2}+\frac{\partial\phi}{\partial z}+W+2\epsilon^2\frac{\partial^2 w}{\partial t\,\partial z}=0 \quad \text{on} \quad z=0. \tag{2.9}$$

We shall investigate the solution for a damped periodic wave correct to $O(\epsilon)$ only.

In studying the time-periodic progressive waves in a long channel, one usually regards the frequency σ as given and real. It is then more convenient to redefine dimensionless variables as follows:

$$\left.\begin{aligned}(x,y,z)=(\sigma^2/g)\,(x',y',z'), \quad t=\sigma t', \\ \mathbf{u}=\mathbf{u}'/\sigma a_0, \quad \phi=\phi'(\sigma/ga_0), \quad \eta=\eta'/a_0.\end{aligned}\right\} \tag{2.10}$$

The dimensionless equations are the same as (2.2)–(2.7) and (2.9) with ϵ interpreted instead as

$$\epsilon=\frac{\sigma^2}{g}\left(\frac{\nu}{\sigma}\right)^{\frac{1}{2}}. \tag{2.11}$$

2.2. *Order estimate in boundary layers*

Boundary layer near a solid wall. While the potential component dominates in the main interior region of the fluid, up to $O(\epsilon)$, within the boundary layer of thickness $O(\epsilon)$ near the solid wall the rotational velocity $\mathbf{U}$ must be added to correct for the no-slip condition. Equation (2.7*a*) shows that the components of the rotational velocity tangential to the solid wall must be of the same order as the potential components namely, $O(\epsilon^0)$. We distinguish by $\mathbf{x}_T$ and x_N the co-ordinates tangential and normal to the wall, respectively; the positive direction of x_N is taken to be from the solid wall *into* the fluid. The boundary-layer nature of $\mathbf{U}$ can then be expressed by assuming

$$\mathbf{U}=\mathbf{U}(\mathbf{x}_T,\zeta,t) \quad \text{with} \quad \zeta=x_N/\epsilon. \tag{2.12}$$

As an immediate consequence, the continuity condition (2.6) becomes approximately (Greenspan 1968, p. 25)

$$-\partial(\mathbf{n}\,.\,\mathbf{U})/\partial\zeta+\epsilon\mathbf{n}\,.\,\nabla\times(\mathbf{n}\times\mathbf{U})=0. \tag{2.13}$$

The unit normal vector $\mathbf{n}$ is pointing *outward* from the fluid. Thus, the component of the rotational velocity normal to the solid wall must be of $O(\epsilon)$. This normal component induces a further adjustment of the potential solution at $O(\epsilon)$.

Free-surface boundary layer. Consider the major part of the free surface excluding the meniscus. In principle a rotational field exists inside the free-surface boundary layer as well. The linearized boundary conditions (2.7*b*–*d*) are to apply at $z=0$. For $ka_0 \gg \epsilon$, i.e. $a_0/\delta \gg 1$, which is often the case in experiments, a proper boundary-layer analysis should be carried out by following a moving curvilinear co-ordinate system with the free surface as a co-ordinate surface. As will now be reasoned, the condition of zero stress on the free surface, however, makes viscosity effective only at $O(\epsilon^2)$, hence to $O(\epsilon)$ we can disregard the boundary-layer structure in the direction normal to the free surface. Consequently the free-surface boundary condition can still be applied at $z = 0$ without the restriction of small a_0/δ. To demonstrate this point, we may imagine that the Lagrangian description is adopted to replace the Eulerian and $\mathbf{x}_0$ is used to designate the position of a fluid particle at $t = t_0$. At all times the true free surface can be taken as $z_0 = 0$, upon which the dynamic boundary condition is applied. For infinitesimal waves, it can be shown that the linearized Navier–Stokes equations in the Lagrangian description are formally the same as those in the Eulerian description, and the boundary-layer analysis can be carried out in the same way (Ünlüata & Mei 1970). In particular (2.7*b*, *c*) still hold for the Lagrangian velocity $\mathbf{U}_L$ with (x, y, z) replaced by (x_0, y_0, z_0) and

$$\mathbf{x} = \mathbf{x}(\mathbf{x}_0, t),$$
$$d\mathbf{x}/dt = \mathbf{u}_L(\mathbf{x}_0, t) = \nabla_L \phi_L(\mathbf{x}_0, t) + \mathbf{U}_L(\mathbf{x}_0, t),$$

where ∇_L denotes the gradient operator with respect to the Lagrangian co-ordinate $\mathbf{x}_0$. Defining a boundary-layer co-ordinate $\zeta_0 = -z_0/\epsilon$ for the rotational part, i.e. $\mathbf{U}_L(\mathbf{x}_0, t) = \mathbf{U}_L(x_0, y_0, \zeta_0, t)$, we have from (2.7*c*) that at $\zeta_0 = 0$

$$\epsilon^2\left(2\frac{\partial^2\phi_L}{\partial x_0\,\partial z_0} + \frac{\partial W_L}{\partial x_0}\right) - \epsilon\frac{\partial U_L}{\partial \zeta_0} = \epsilon^2\left(2\frac{\partial^2\phi_L}{\partial y_0\,\partial z_0} + \frac{\partial W_L}{\partial y_0}\right) - \epsilon\frac{\partial V_L}{\partial \zeta_0} = 0. \tag{2.14}$$

Therefore $\partial(U_L, V_L)/\partial\zeta_0 = O(\epsilon)$ and $U_L, V_L = O(\epsilon)$ since (U_L, V_L) vanish outside the boundary layer. From continuity $W_L = O(\epsilon^2)$; it then follows from (2.9) that

$$\partial^2\phi_L/\partial t^2 + \partial\phi_L/\partial z_0 = O(\epsilon^2).$$

In other words, viscosity is ineffective on the free surface at $O(\epsilon)$. Since

$$\mathbf{x} - \mathbf{x}_0 = O(ka_0),$$

the Eulerian and Lagrangian velocity fields differ only by $O(ka_0)$. The above equation therefore implies that the Eulerian field is also subject to the condition

$$\partial^2\phi/\partial t^2 + \partial\phi/\partial z = O(\epsilon^2) \quad \text{on} \quad z = 0. \tag{2.15}$$

Free-surface meniscus. The corner region where the side-wall and free-surface layers overlap deserves special care. For simplicity we shall assume that near $z = 0$ the wall is vertical, see figure 1. Since the viscous effect in the free-surface layer is absent up to the outer edge of the side-wall layer, and the boundary conditions on the wall do not imply any fast changes in the vertical direction, the boundary-layer behaviour in this corner is only significant in the direction normal to the wall, i.e. $\partial/\partial x, \partial/\partial y \gg \partial/\partial z$. In particular, the rotational part of the vertical velocity varies quickly from $[-\partial\phi/\partial z]_{z=0}$ at the wall to zero within a horizontal distance of $O(\epsilon)$ away from the wall. In other words, within this width (and only within it) W is of $O(\epsilon^0)$. Thus from (2.9), we have

$$\partial^2\phi/\partial t^2 + \partial\phi/\partial z = -W \quad \text{on} \quad z = 0. \tag{2.16}$$

Equation (2.16) applies over the entire surface $z = 0$ in view of (2.15) and the fact that $W \to 0$ as $\zeta \to \infty$. Now the rotational velocity W acts as an equivalent pressure to the potential field. It is of $O(1)$ in magnitude, nevertheless it is non-zero only within a narrow belt of area of $O(\epsilon)$. Therefore its integrated effect is

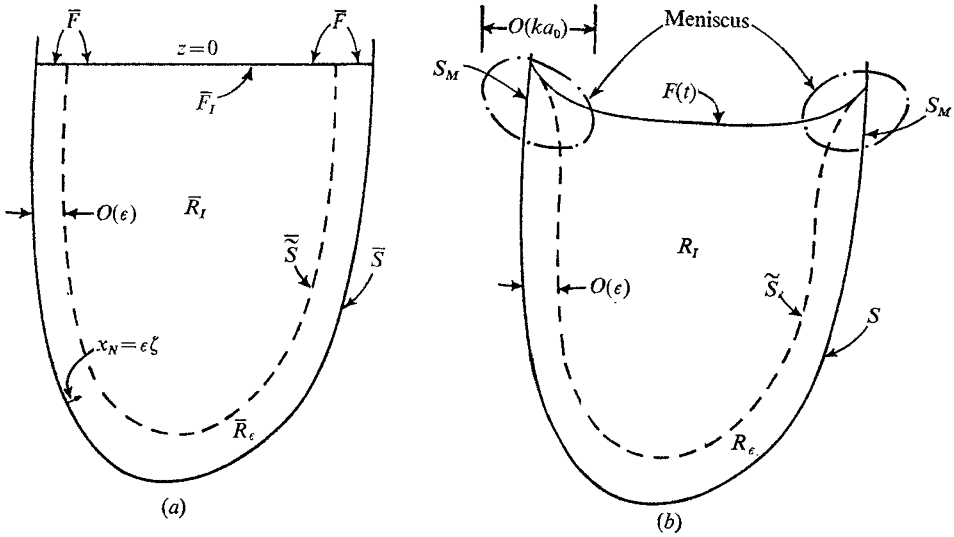

FIGURE 1. Division of fluid regions. (*a*) Mean control volumes defined by the mean free surface $\bar{F}$ at $z = 0$. (*b*) Instantaneous control volumes defined by the instantaneous free surface $F(t)$. Dashed lines show the outer surface of boundary layer. Since dimension of meniscus $= O(ka_0)$, $(R_I, R_\epsilon, S, \tilde{S}) = (\bar{R}_I, \bar{R}_\epsilon, \bar{\tilde{S}},)\,(1+O(ka_0))$.

of significance only at $O(\epsilon)$. It indeed behaves like a singular concentrated forcing function at the rim of the free surface. This is an important point and the physical picture will be further elucidated later.

2.3. *Perturbation analysis*

Standing waves. For standing waves in a basin with mean rigid boundary $\bar{S}$ and mean free surface $\bar{F}$ ($z = 0$), see figure 1, we seek perturbation expansions as follows:

$$\left.\begin{aligned} \phi &= [\phi_0(\mathbf{x})+\epsilon\phi_1(\mathbf{x})+O(\epsilon^2)]\,e^{i\sigma t},\\ \mathbf{U} &= [\mathbf{q}_0(\mathbf{x}_T,\zeta)+\epsilon\mathbf{q}_1(\mathbf{x}_T,\zeta)+O(\epsilon^2)]\,e^{i\sigma t},\\ \sigma &= \sigma_0+\epsilon\sigma_1+O(\epsilon^2). \end{aligned}\right\} \tag{2.17}$$

Substituting into (2.4)–(2.9), a sequence of problems results.

(1) Inviscid solution of $O(\epsilon^0)$:

$$\nabla^2\phi_0 = 0, \tag{2.18a}$$

$$\mathbf{n}\,.\,\nabla\phi_0 = 0 \quad \text{on} \quad \bar{S}, \tag{2.18b}$$

$$\partial\phi_0/\partial z-\sigma_0^2\phi_0 = 0 \quad \text{on} \quad \bar{F}, z = 0. \tag{2.18c}$$

(2) Boundary-layer correction of $O(\epsilon^0)$:

$$\partial^2\mathbf{q}_0/\partial\zeta^2 = i\sigma_0\mathbf{q}_0, \tag{2.19a}$$

$$\mathbf{q}_0 = -\nabla\phi_0 \quad \text{on} \quad \bar{S}, \quad \zeta = 0, \tag{2.19b}$$

$$\mathbf{q}_0 \to 0 \quad \text{as} \quad \zeta\to\infty. \tag{2.19c}$$

Note that $\mathbf{q}_0$ is tangential to the surface $\bar{S}$. The continuity equation (2.6) gives

$$-\partial(\mathbf{n}\,.\,\mathbf{q}_1)/\partial\zeta+\mathbf{n}\,.\,\nabla\times(\mathbf{n}\times\mathbf{q}_0) = 0, \tag{2.20}$$

from which the normal component $\mathbf{n}.\mathbf{q}_1$ may be obtained by integration subject to the boundary condition $\mathbf{n}.\mathbf{q}_1 \to 0$ as $\zeta \to \infty$. Finally, this normal component does not vanish on $\bar{S}$ ($\zeta = 0$) and induces a further adjustment of the interior solution.

(3) Inviscid solution of $O(\epsilon)$:

$$\nabla^2\phi_1 = 0, \tag{2.21a}$$

$$\mathbf{n}.\nabla\phi_1 = -[\mathbf{n}.\mathbf{q}_1]_{\bar{S}} \quad \text{on} \quad \bar{S}, \tag{2.21b}$$

$$\partial\phi_1/\partial z - \sigma_0^2\phi_1 = 2\sigma_0\sigma_1\phi_0 - W_0/\epsilon \quad \text{on} \quad \bar{F} \quad (z = 0), \tag{2.21c}$$

where $[\ ]_{\bar{S}}$ represents a quantity evaluated at the solid wall. Recall that W_0 is the vertical component of the first-order, $O(\epsilon^0)$, rotational velocity in the main side-wall boundary layer. Owing to the narrow $O(\epsilon)$ region of its existence its effect is only present in the $O(\epsilon)$ problem as was discussed in §2.2.

Problem 1 is homogeneous and its standing-wave solution including the eigenvalue condition for σ_0 (dispersion relation) can be found in principle. Problem 2 is the classical Stokes problem of an oscillating plate with the well-known solution

$$\mathbf{q}_0 = -[\nabla\phi_0]_{\bar{S}}\,\Gamma(\zeta), \quad \Gamma(\zeta) = \exp[-(1+i)(\tfrac{1}{2}\sigma_0)^{\frac{1}{2}}\zeta]. \tag{2.22}$$

Now problem 3 is inhomogeneous. Upon using Green's second identity for ϕ_0^* and ϕ_1 for the whole volume $\bar{R}$,

$$\int_{\bar{R}} (\phi_0^*\nabla^2\phi_1 - \phi_1\nabla^2\phi_0^*)\,dV = \int_{\bar{S}+\bar{F}} (\phi_0^*\nabla\phi_1 - \phi_1\nabla\phi_0^*)\,\mathbf{n}.d\mathbf{A},$$

and applying all the conditions (2.18) and (2.21), we obtain a solvability condition for ϕ_1 which determines σ_1:

$$\begin{aligned}\sigma_1 &= \left\{\int_{\bar{S}} \phi_0^*[\mathbf{n}.\mathbf{q}_1]_{\bar{S}}\,dA + \int_{\bar{F}} \phi_0^*\,W_0\,dA/\epsilon\right\}\Big/ 2\sigma_0\int_{\bar{F}} |\phi|^2\,dA \\ &= \sigma_0\left\{\int_{\bar{S}} \phi_0^*[\mathbf{n}.\mathbf{q}_1]_{\bar{S}}\,dA + \int_{\bar{F}} \phi_0^*\,W_0\,dA/\epsilon\right\}\Big/ 2\int_{\bar{R}} |\nabla\phi_0|^2\,dV.\end{aligned} \tag{2.23}$$

The alternative expressions are equivalent by virtue of Gauss's theorem and (2.18*c*). By taking the real and imaginary parts, the frequency change $\mathrm{Re}\,(\epsilon\sigma_1)$ and the damping factor $\mathrm{Im}\,(\epsilon\sigma_1)$ are found. The imaginary part of the integrals in the numerator in (2.23) may be shown to represent the average rates of pressure working: the first through the outer edge of wall boundary layer (side walls and bottom) and the second through the narrow strip of free surface bounding the side-wall layer from above. Since the denominator is essentially the energy in the inviscid core, physically $\mathrm{Im}\,\sigma = \mathrm{Im}\,(\epsilon\sigma_1)$ represents the ratio of the work done by the interior on the boundary layer to the total energy in the main body of the fluid.

Progressive waves in a channel. For progressive waves in a straight channel of uniform cross-section we first assume that the wavenumber k is real and that the time rate of attenuation is wanted. Instead of (2.17) we take the following expansions:

$$\phi = [\phi_0(y,z) + \epsilon\phi_1(y,z) + O(\epsilon^2)]\,e^{i(\sigma t - x)}, \tag{2.24a}$$

$$\mathbf{U} = [\mathbf{q}_0(\mathbf{x}_T,\zeta) + \epsilon\mathbf{q}_1(\mathbf{x}_T,\zeta) + O(\epsilon^2)]\,e^{i(\sigma t - x)}, \tag{2.24b}$$

$$\sigma = \sigma_0 + \epsilon\sigma_1 + O(\epsilon^2), \tag{2.24c}$$

where the x axis coincides with the channel axis. The characteristic k used in (2.1) is the physical wavenumber in the x direction. Upon substitution the resulting problems are almost the same as (2.18), (2.19) and (2.21) except that $\mathbf{n}$ lies in the y, z plane and the Laplace equation for the inviscid problems (1 and 3) must be replaced by

$$\left(\frac{\partial^2}{\partial y^2}+\frac{\partial^2}{\partial z^2}-1\right)\phi_m = 0 \quad (m = 0, 1, \ldots). \tag{2.25}$$

With these modifications the result (2.23) is again valid. The surface and volume integrations are for a region length one unit in the x direction.

Alternatively, if the frequency is assumed real and fixed the change in wavenumber can be inferred from σ_1 above through the group velocity. One could also begin by adopting the dimensionless variables defined in (2.10) with ϵ defined by (2.11), and replace the exponential factor in the expansions of (2.24a, b) by $e^{i(kx-t)}$ with

$$k = k_0+\epsilon k_1+\ldots \tag{2.26}$$

replacing (2.24c). Similar perturbation analysis then gives

$$k_1 = \left\{-\int_{\bar{S}}\phi_0^*[\mathbf{n}.\mathbf{q}_1]_{\bar{S}}\,dA-\int_{\bar{F}}\phi_0^*\,W_0\,dA/\epsilon\right\}\Big/2k_0\int_{\bar{R}}|\phi_0|^2\,dV. \tag{2.27}$$

3. Mechanism of energy transfer

Our purpose here is to examine the energy budget within various fluid regions so that the process of energy transfer is clearly revealed. The common approach of attributing wave decay to viscous dissipation amounts to a special choice of the region, i.e. the entire fluid volume. A detailed look at the side-wall boundary layer and the free-surface meniscus brings the path of energy flow into a much sharper focus. In particular, we shall find by order estimates that the free-surface meniscus is an important passage via which the wave energy is lost from the essentially inviscid interior to the side-wall boundary layer. This discussion is therefore relevant to the physical nature of Ursell's singularity. In the next section these estimates are substantiated explicitly for special examples.

We first quote the equation of mechanical energy. Take a volume $\mathscr{V}$ which is bounded by the surface $\mathscr{A}$. In physical variables the mechanical energy equation in integral form is (Landau & Lifshitz 1959, p. 54)

$$\int_{\mathscr{V}}\frac{\partial}{\partial t'}(\tfrac{1}{2}\rho u_i'u_i')\,dV' = \int_{\mathscr{A}}(-\tfrac{1}{2}\rho u_i'u_j'u_j'+\tau_{ij}'u_j')\,n_i\,dA' + \int_{\mathscr{A}}p'u_i'n_i\,dA'+\int_{\mathscr{V}}\rho g_i u_i'\,dV'-\frac{1}{2\mu}\int_{\mathscr{V}}\tau_{ij}'^2\,dV', \tag{3.1}$$

where
$$\tau_{ij}' = \mu\left(\frac{\partial u_i'}{\partial x_j'}+\frac{\partial u_j'}{\partial x_i'}\right) \equiv \mu\, e_{ij}' \tag{3.2}$$

is the viscous stress tensor, e_{ij}' the strain tensor, $(x_1', x_2', x_3') = (x', y', z')$ and g_i is the body force of gravity: $g_{1,2} = 0$ and $g_3 = -g$. For small amplitude waves,

$ka_0 \ll 1$, the energy flux term in the first surface integral is of $O(ka_0)^3$ and can be ignored in comparison with the remaining terms of $O(ka_0)^2$. Writing

$$g_i = -\partial(gz')/\partial x_i'$$

and using Gauss's theorem we have

$$-\int_{\mathscr{A}} p'u_i'n_i\,dA + \int_{\mathscr{V}} \rho g_i u_i'\,dV' = -\int_{\mathscr{A}} p'u_i'n_i\,dA - \int_{\mathscr{A}} \rho g z' u_i' n_i\,dA'$$

$$= -\int_{\mathscr{A}} p_d' u_i' n_i\,dA',$$

where $p_d' = p' + gz'$ is the dynamic pressure.

Taking time averages defined by

$$\bar{f} = \frac{1}{T}\int_{t'}^{t'+T} f\,dt', \quad T = 2\pi/\mathrm{Re}\,\sigma, \tag{3.3a}$$

so that

$$\overline{\partial f/\partial t} = \partial\bar{f}/\partial t, \tag{3.3b}$$

and adopting the dimensionless variables (2.1), the approximate mechanical energy equation reads

$$\overline{\int_{\mathscr{V}} \frac{\partial}{\partial t}(\tfrac{1}{2}u_i u_i)\,dV} = -\overline{\int_{\mathscr{A}} p_d u_i n_i\,dA} + \epsilon^2 \overline{\int_{\mathscr{A}} e_{ij} u_j n_i\,dA} - \tfrac{1}{2}\epsilon^2 \overline{\int_{\mathscr{V}} e_{ij}^2\,dV}. \tag{3.4}$$

$$\text{(I)} \qquad\qquad \text{(II)} \qquad\qquad \text{(III)} \qquad\qquad \text{(IV)}$$

Physically the terms represent respectively the rate of change of kinetic energy (I), the rate of pressure working (II), the rate of viscous stress working (III) and the rate of dissipation (IV). We divide the entire volume of fluid as in figure 1 into the inviscid interior R_I, the wall boundary layer R_ϵ and the meniscus R_M. The solid faces of the boundary layers are denoted by S and S_M and the corresponding outer edges of the layers by $\tilde{S}$ and $\tilde{S}_M$. For generality it is assumed that $a_0/\delta \gg 1$. In the neighbourhood of the meniscus the free surface attains its greatest height at the level M and least height at the level A. At any instant the free surface MED must begin at the fixed point M above which the wall is not wetted. The piece of free surface ME of the meniscus changes from being nearly horizontal at the maximum rise to being a thin film at the maximum fall. At any intermediate time during each period the meniscus consists of a thin viscous boundary layer MAB of thickness of $O(\epsilon)$ and height of $O(ka_0)$ near the wall and a potential region whose boundary and volume change with time. The lower extreme of this boundary layer AB also forms the ceiling of the main wall boundary layer R_ϵ. We shall consider in succession the energy budget of the entire fluid volume, the meniscus boundary layer and lastly the inviscid core, being the total volume minus all the boundary layers.

We now sort out the leading terms in (3.4) for different control volumes.

3.1. *The entire fluid*

Let the volume $\mathscr{V}$ be the entire fluid volume R, hence the boundary surface consists of all wetted walls and the free surface F:

$$\mathscr{V} = R_I + R_\epsilon + R_M, \quad \mathscr{A} = S + S_M + F.$$

Referring to (3.4) term I is well approximated by

$$\frac{1}{2}\frac{\partial}{\partial t}\int_{R_I}\overline{u_i u_i}\,dV$$

since $R_I = O(1) \gg R_\epsilon + R_M = O(\epsilon)$, and $u_i = O(1)$ in all regions. We anticipate that the time rate of change of all mean quantities is $\partial\overline{(\;)}/\partial t = O(\epsilon)$ hence term I $= O(\epsilon)$.

For term II, $u_i n_i = 0$ on the solid wall $S + S_M$ but not on the free surface F. The contribution of the meniscus free surface (ME) is certainly negligible compared with (being $O(ka_0)$ smaller than) that of the main free surface away from the meniscus. Furthermore on the main free surface viscosity is ineffective, $p_d = [-\partial\phi/\partial t]_{z=0} = \eta$ and $u_i n_j = w = \eta$, so the integral can be written as

$$\overline{\int_F p_d u_i n_i\,dA} = \int_{\bar{F}}\overline{p_d w}\,dA + O(ka_0) = \frac{\partial}{\partial t}\int_{\bar{F}}\tfrac{1}{2}\overline{\eta^2}\,dA + O(ka_0),$$

where $\bar{F}$ denotes the mean free surface $z = 0$. The last expression represents the change of potential energy of the free surface and is of course also of $O(\epsilon)$. Hence term II $= O(\epsilon)$.

Term III vanishes on $S + S_M$ since $u_i = 0$; and also on F since the free surface is stress-free: $e_{ij} n_i = 0$.

Term IV $= O(\epsilon)$ in the boundary layers since $e_{ij} = O(\epsilon^{-1})$ and $R_\epsilon + R_M = O(\epsilon)$. The contribution from the essentially inviscid interior is of $O(\epsilon^2)$. Furthermore, the volume of the meniscus boundary layer is much smaller than the volume of the wall boundary layer, $R_M/R_\epsilon = O(ka_0)$, while the straining rate is of the same order. Hence we need only to account for the dissipation in the main wall boundary layer. Summing up we have to $O(\epsilon)$

$$\frac{\partial}{\partial t}\left\{\int_{R_I}\tfrac{1}{2}\overline{u_i u_i}\,dV + \int_{\bar{F}}\tfrac{1}{2}\overline{\eta^2}\,dA\right\} = -\tfrac{1}{2}\epsilon^2\int\overline{e_{ij}^2}\,dV, \tag{3.5}$$

which is the basis of many existing damping theories.

3.2. *Meniscus boundary layer*†

Now consider the meniscus boundary layer with volume $\mathscr{V} = R_M$ and bounding surface $\mathscr{A} = S_M + \tilde{S}_M + S_{MW}$, where S_M is the side wall, $\tilde{S}_M$ the outer edge of the boundary layer and S_{MW} the borderline with the main wall layer, see figure 2. Referring to (3.4) we find the following.

Term I. $u_i = O(1)$ and $R_M = O(\epsilon ka)$ hence

$$\text{term I} = O\left(\frac{\partial}{\partial t}\overline{\int_{R_M} u_i u_i\,dV}\right).$$

Since $\partial\overline{(\;)} = O(\epsilon)$, term I $= O(\epsilon^2 ka)$.

Term II. S_M gives no contribution since $u_i = 0$. On S_{MW}, $u_i n_i = w = O(1)$, $p_d = O(1)$ and $S_{MW} = O(\epsilon)$, hence the integral over S_{MW} is of $O(\epsilon)$. On the outer edge $\tilde{S}_M$ of the meniscus boundary layer the tangential velocity is $w = O(1)$.

† Comments by Professor G. K. Batchelor during a lecture given by one of the authors have led to the arguments in this section.

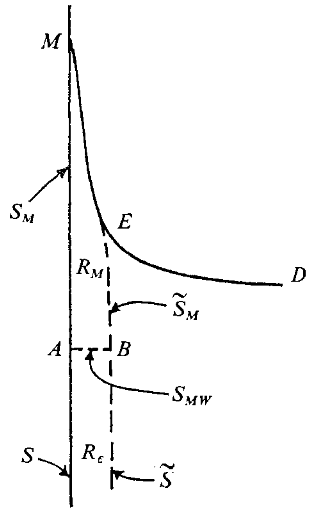

FIGURE 2. Enlarged view of meniscus neighbourhood. The line AB (S_{MW}) symbolizes border between meniscus and main wall boundary layers.

Note that the tangential (vertical) length scale is of $O(ka_0)$. Hence by continuity the normal (horizontal) velocity is $u_i n_i = O(\epsilon/ka_0)$. Since $p_d = -\phi_t = O(1)$ and the area of $\tilde{S}_M$ is of $O(ka_0)$ we have

$$\int_{\tilde{S}_M} \overline{p_d u_i n_i}\, dA = O(\epsilon).$$

Term III. On S_M, $u_i = 0$. On $\tilde{S}_M$, $e_{ij} = O(1)$. The integral on $S_M + \tilde{S}_M$ is of $O(\epsilon^2 ka_0)$. On S_{MW}, $e_{ij} = O(\epsilon^{-1})$ and $u_i = O(1)$, and the area of $S_{MW} = O(\epsilon)$, hence the integral is only of $O(\epsilon^2)$.

Term IV. As was estimated before the dissipation rate in this volume is of $O(\epsilon ka_0)$.

Thus to $O(\epsilon)$

$$\overline{\int_{\tilde{S}_M} p_d u_i n_i\, dA} + \int_{\tilde{S}_{MW}} \overline{p_d u_i n_i}\, dA = O(\epsilon^2), \tag{3.6}$$

which means that, by pressure working on $\tilde{S}_M$, power is fed into the meniscus boundary layer from the inviscid core; it is then transmitted essentially undiminished to the main wall boundary layer also through pressure working on S_{MW}. This is an important source of energy supply for the main side-wall layer!

3.3. *Wall boundary layer*

Take the wall layer bounded by the solid surface S, the outer edge of the boundary layer $\tilde{S}$ and the narrow strip bordering the free-surface menicous boundary layer S_{MW}. Similar estimates give that term I $= O(\epsilon^2)$, term II $= O(\epsilon)$, term III $= O(\epsilon^2)$ and term IV $= O(\epsilon)$. In particular the pressure working term has contributions from both $\tilde{S}$ and S_{MW}. The resulting energy budget is, to $O(\epsilon)$, given by

$$-\int_{S_{MW}} \overline{p_d w}\, dA - \int_{\tilde{S}} \overline{p_d u_i n_i}\, dA - \tfrac{1}{2}\epsilon^2 \int_{R_\epsilon} \overline{e_{ij}^2}\, dV = 0, \tag{3.7}$$

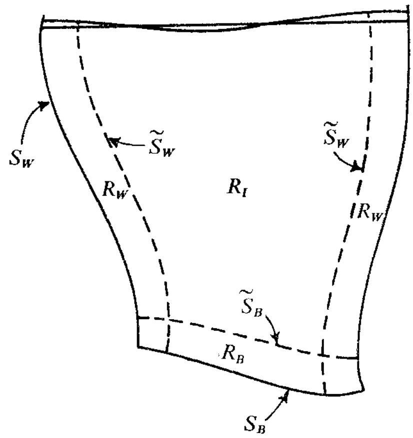

FIGURE 3. Container with bottom corners. Main wall boundary layer R_ϵ is separated into side-wall R_W and bottom R_B layers; $R_\epsilon = R_W + R_B$.

namely pressure working on the ceiling and on the side balances the dissipation within.

If the container has sharp convex corners below the free surface it is convenient to separate the wall layer into a side-wall layer R_W and a bottom layer R_B. The transition zones are corners of area of $O(\epsilon^2)$, see figure 3. Since at a corner of this kind the irrotational field has a stagnation point, all surface and volume integrals in (3.4) associated with the corner are at most of $O(\epsilon^2)$ and can be ignored. Thus the energy budget for the bottom boundary layer is

$$-\int_{\tilde{S}_B} \overline{p_d u_i} n_i \, dA - \tfrac{1}{2}\epsilon^2 \int_{R_B} \overline{e_{ij}^2} \, dV = O(\epsilon^2), \tag{3.8}$$

i.e. dissipation within R_B is balanced by pressure working on the side $\tilde{S}_B$ (not at the corners) by the inviscid core.

3.4. *Interior core*

Finally we take the inviscid core $\mathscr{V} = R_I$ with bounding surface

$$\mathscr{A} = S_W + S_M + F_I.$$

It is easily shown that term I $= O(\epsilon)$, term II $= O(\epsilon)$, term III $= O(\epsilon^2)$, since $e_{ij}, u_j = O(1)$, and term IV $= O(\epsilon^2)$. Furthermore, of all the surface integrals contributing to term II, the free-surface integral can be transformed into the potential energy as before. Hence

$$\frac{\partial}{\partial t}\left\{\int_{R_I} \tfrac{1}{2}\overline{u_i u_i} \, dV + \int_{F_I} \tfrac{1}{2}\overline{\eta^2} \, dA\right\} = -\int_{\tilde{S}+\tilde{S}_M} \overline{p_d u_i} n_i \, dA + O(\epsilon^2).$$

Now on the left-hand side R_I and F_I may be replaced by their mean counterparts $\bar{R}$ and $\bar{F}$ with an error of $O(\epsilon k a_0, \epsilon^2)$. Finally

$$\frac{\partial}{\partial t}\left\{\int_{\bar{R}} \tfrac{1}{2}\overline{u_i u_i} \, dV + \int_{\bar{F}} \tfrac{1}{2}\overline{\eta^2} \, dA\right\} = -\int_{\tilde{S}+\tilde{S}_M} \overline{p_d u_i} n_j \, dA, \tag{3.9}$$

expressing the energy budget for the inviscid core. It is clear that (3.5), (3.6), (3.7) and (3.9) are totally consistent. Upon using (3.6) we can also write (3.9) as

$$\frac{\partial}{\partial t}\left\{\int_R \tfrac{1}{2}\overline{u_i u_i}\,dV+\int_F \tfrac{1}{2}\overline{\eta^2}\,dA\right\}=-\int_{\tilde{S}}\overline{p_d u_i n_i}\,dA-\int_{S_{MW}}\overline{p_d w}\,dA. \quad (3.10)$$

3.5. *The damping rate*

It is now easy to re-derive the damping rate (2.23) from (3.10). As a slight modification of a well-known formula, it can be shown that if

$$a_l(t)=\mathrm{Re}\,[A_l \exp\{i(\sigma^{(r)}+i\sigma^{(i)})\,t\}] \quad (3.11)$$

with

$$\sigma^{(i)}/\sigma^{(r)}=O(\epsilon), \quad (3.12)$$

then

$$\begin{aligned}\overline{a_l a_m}&=\tfrac{1}{2}\,\mathrm{Im}\,(iA_l^* A_m)\exp\{-2\sigma^{(i)}t\}\,[1+O(\epsilon)]\\&=\tfrac{1}{2}\,\mathrm{Re}\,(A_l^* A_m)\exp\{-2\sigma^{(i)}t\}\,[1+O(\epsilon)].\end{aligned} \quad (3.13)$$

The left-hand side of (3.10) involves only potential quantities hence the equipartition theorem may be used. On the right-hand side the following is true:

$$[p_d]_{\tilde{S}}=-[\partial\phi/\partial t]_{\tilde{S}}=(-\sigma_0\phi_0)_S\,e^{i\sigma t}+O(\epsilon),$$

$$[p_d]_{S_{MW}}=(-i\sigma_0\phi_0)_{S,z=0}\,e^{i\sigma t}+O(\epsilon),$$

$$[u_i n_i)_{\tilde{S}}=[\mathbf{n}\,.\,\nabla\phi]_{\tilde{S}}=-[\mathbf{n}\,.\,\mathbf{q}_1]_S\,e^{i\sigma t}+O(\epsilon^2),$$

and in view of (2.21*b*). Upon substitution we have

$$-2\sigma^{(i)}\int_R|\nabla\phi_0|^2\,dV=\epsilon\,\mathrm{Im}\left\{i\left[\int_S(-i\sigma_0\phi_0)^*\,[\mathbf{n}\,.\,\mathbf{q}_1]_S\,dA-\int_{S_{MW}}(-i\sigma_0\phi_0)_{\tilde{S}}^*\,W_0\,dA/\epsilon\right]\right\}$$

or

$$\mathrm{Im}\,\sigma_1=\sigma^{(i)}/\epsilon=\frac{\mathrm{Im}\left\{\sigma_0\left[\int_S\phi_0^*[\mathbf{n}\,.\,\mathbf{q}_1]_S\,dA+\int_{S_{MW}}\phi_0^*\,W_0\,dA/\epsilon\right]\right\}}{2\int_R|\nabla\phi_0|^2\,dV}. \quad (3.14)$$

Without loss of accuracy the area of integration for the first integral in the numerator can be replaced by $\overline{S}$ and that for the second integral by $\overline{F}$ $(z=0)$. This result for the damping rate is in agreement with (2.23), deduced by the mathematical requirement of solvability for ϕ_1.

The arguments in the present section rely on order-of-magnitude estimates. The special examples in the following section not only confirm them but also give further insight into the energy transfer.

4. Examples

The complex frequency shift is worked out for three familiar examples, all of which involve vertical side walls.

4.1. *Standing waves in a circular basin*

The origin of the polar co-ordinate system is fixed at the centre of the free surface; the radius of the basin is a' and the depth h'.

As only one mode will be considered below, we choose the scaling wavenumber k (cf. (2.1)) to be that of the (m,n) mode, k_{mn}, i.e. the mth root of the equation

$$J_n'(k_{mn}a') = 0 \quad (n, m = 1, 2, 3, \ldots), \tag{4.1}$$

where $J_n' = dJ_n(z)/dz$.

The first-order inviscid solution for the (m,n) mode is

$$\phi_0 = i\sigma_0(\sinh h)^{-1}\cosh(z+h)\,J_n(r)\sin n\theta, \tag{4.2}$$

where

$$\sigma_0^2 = \tanh h. \tag{4.3}$$

Let U, V and W denote the components of the rotational velocity in the r, θ and z directions, respectively. We divide the wall boundary layer into two parts, i.e. the side-wall and the bottom layer, denoted by subscripts W and B respectively, and let the boundary-layer co-ordinates be

$$\zeta_W = (a-r)/\epsilon, \quad \zeta_B = (z+h)/\epsilon. \tag{4.4a,b}$$

The first-order boundary-layer solutions are

$$U_{0W} = 0, \tag{4.5a}$$

$$V_{0W} = -i\sigma_0\frac{n}{a}J_n(a)\frac{\cosh(z+h)}{\sinh h}\cos n\theta\,\Gamma(\zeta_W), \tag{4.5b}$$

$$W_{0W} = -i\sigma_0 J_n(a)\frac{\sinh(z+h)}{\sinh h}\sin n\theta\,\Gamma(\zeta_W) \tag{4.5c}$$

in the neighbourhood of the side wall and

$$U_{0B} = \frac{-i\sigma_0}{\sinh h}J_n'(r)\sin n\theta\,\Gamma(\zeta_B), \tag{4.6a}$$

$$V_{0B} = \frac{-i\sigma_0}{\sinh h}\frac{n}{r}J_n(r)\cos n\theta\,\Gamma(\zeta_B), \tag{4.6b}$$

$$W_{0B} = 0 \tag{4.6c}$$

in the neighbourhood of the bottom with $\Gamma(\zeta)$ defined in (2.22). The induced velocities normal to the boundary layers are

$$\begin{aligned} U_{1W} &= \int_\infty^{\zeta_W}\left(\frac{1}{a}\frac{\partial V_{0W}}{\partial\theta}+\frac{\partial W_{0W}}{\partial z}\right)d\zeta_W \\ &= -(1+i)\left(\frac{\sigma_0}{2}\right)^{\frac{1}{2}}\left(\frac{n^2}{a^2}-1\right)\frac{\cosh(z+h)}{\sinh h}\sin n\theta\,J_n(a)\,\Gamma(\zeta_W) \end{aligned} \tag{4.7}$$

near the side wall and

$$\begin{aligned} W_{1B} &= \int_\infty^{\zeta_B}\left(\frac{\partial U_{0B}}{\partial r}+\frac{U_{0B}}{r}+\frac{1}{r}\frac{\partial V_{0B}}{\partial\theta}\right)d\zeta_B \\ &= (1+i)\left(\frac{\sigma_0}{2}\right)^{\frac{1}{2}}\frac{\sin n\theta}{\sinh h}J_n(r)\,\Gamma(\zeta_B) \end{aligned} \tag{4.8}$$

near the bottom.

Substituting into (2.23) we obtain

$$\sigma_1 = -(1-i)\left(\frac{\sigma_0}{2}\right)^{\frac{1}{2}}\left[\frac{a^2+n^2}{2a(a^2-n^2)}+\left(1-\frac{h}{a}\right)\frac{1}{\sinh 2h}\right], \tag{4.9}$$

whose imaginary part agrees with the damping rate found by Case & Parkinson (1957).

It is interesting to examine the energy details for the side-wall boundary layer, using the explicit solution.

The average work done by the pressure on the strip of surface S_{MW} is, omitting the factor $\exp\{-2\sigma^{(i)}t\}$,

$$\operatorname{Re}\int_0^{2\pi} a\,d\theta\int_0^{\infty}[p_{d_0}^*]_{z=0,r=a}[w]_{z=0}\,d\zeta_W = \operatorname{Re} a\int_0^{2\pi} d\theta\,[i\sigma_0\phi_0^*]_{z=0,r=a}\int_0^{\infty}[W_{0W}]_{z=0}\,d\zeta_W$$

$$= -\pi a\left(\frac{\sigma_0}{2}\right)^{\frac{1}{2}} J_n^2(a), \tag{4.10}$$

where use has been made of the fact that the dynamic pressure and the potential part of the velocity are out of phase to the present order of approximation. The work done by the pressure on the interface between the inviscid interior and the side-wall layer is (noting that the outward normal points towards the z axis)

$$\operatorname{Re}\int_h^0 dz\int_0^{2\pi} a\left[p_{d_0}^*\left(-\frac{\partial\phi_1}{\partial r}\right)\right]_{r=a} d\theta = \operatorname{Re}\int_{-h}^0 dz\int_0^{2\pi} a[i\sigma_0\phi_0^*\,U_{1W}]_{r=a}\,d\theta$$

$$= -\frac{\pi a}{2}\left(\frac{\sigma_0}{2}\right)^{\frac{1}{2}}\left(1+\frac{2h}{\sinh 2h}\right)\left(\frac{n^2}{a_2}-1\right)J_n^2(a). \tag{4.11}$$

Lastly, the average rate of viscous dissipation in the side-wall layer is

$$\operatorname{Re}\int_{-h}^0 dz\int_0^{2\pi} a\,d\theta\int_0^{\infty}\left(\left|\frac{\partial V_{0W}}{\partial\zeta_W}\right|^2+\left|\frac{\partial W_{0W}}{\partial\zeta_W}\right|^2\right)d\zeta_W$$

$$= \pi a\left(\frac{\sigma_0}{2}\right)^{\frac{1}{2}} J_n^2(a)\left[\frac{1}{2}\left(\frac{n^2}{a^2}-1\right)\left(1+\frac{2h}{\sinh 2h}\right)+1\right]. \tag{4.12}$$

It is easily seen that the three energy terms (4.10)–(4.12) add up precisely to zero as estimated in (3.6).

Since $n^2 < a^2 = (k_{mn}a')^2$ for all modes, it follows that the side-wall layer receives power from waves through the meniscus boundary layer above, spends only a part of it on internal dissipation and gives up the rest to the inviscid interior!

Similar calculation for the bottom layer confirms (3.8), with no surprises.

4.2. *Standing waves in a rectangular basin*

We have also analysed standing waves in a cylindrical basin of rectangular plan form. For the (m,n) mode, the first-order potential is given by

$$\phi_0 = \frac{i\sigma_0}{\sinh h}\cosh(z+h)\cos\frac{n\pi x}{a}\cos\frac{m\pi y}{b}, \tag{4.13a}$$

$$\sigma_0^2 = \tanh h, \tag{4.13b}$$

where the scaling k is the wavenumber k_{mn} of the (m,n) mode, satisfying

$$k_{mn}^2 = (n\pi/a')^2+(m\pi/b')^2 \tag{4.14}$$

for a tank of length $2a'$, width $2b'$ and depth h'. The total frequency change is

$$\sigma_1 = -(1-i)\left(\frac{\sigma_0}{2}\right)^{\frac{1}{2}}\left\{\frac{1}{a}\left[1-\frac{1}{2}\left(\frac{n\pi}{a}\right)^2\right]+\frac{1}{b}\left[1-\frac{1}{2}\left(\frac{m\pi}{b}\right)^2\right] + \frac{1}{\sinh 2h}\left[1-\frac{h}{a}\left(\frac{n\pi}{a}\right)^2-\frac{h}{b}\left(\frac{m\pi}{b}\right)^2\right]\right\}. \quad (4.15)$$

Keulegan (1959) worked out the damping rate for $n = 1$ and $m = 0$, which agrees with the imaginary part above. The energy budget has been checked as in the circular cylinder case with similar conclusions.

4.3. *Plane progressive waves in a uniform channel of rectangular cross-section*

The centre-line of the free surface is taken to be the x axis of the rectangular co-ordinate system; the channel width is $2b'$ and the depth h'.

For simplicity the first-order inviscid solution ϕ_0 is assumed to represent a plane wave with uniform amplitude across the channel hence $\phi_0 = \phi_0(z)$ is independent of y (although waves with width-wise variation can be treated without difficulty). This is the most frequent situation encountered in laboratory experiments. The first-order potential solution is well known:

$$\phi_0 = i\sigma_0 \cosh(z+h)/\sinh h \quad (4.16)$$

with $$\sigma_0^2 = \tanh h.$$

The frequency change is, from (2.23),

$$\sigma_1 = -(1-i)\left(\frac{\sigma_0}{2}\right)^{\frac{1}{2}}\left(\frac{1}{\sinh 2h}+\frac{1}{b}\right). \quad (4.17)$$

By straightforward calculations similar to (4.10)–(4.12), it is found that in the bottom boundary layer the dissipation is balanced by pressure working by the inviscid interior. However, owing to the two-dimensional nature of the first-order potential, there is no rotational velocity component induced normal to the side-wall boundary layers. This is seen from the following relation for the left side wall ($y \sim b$):

$$V_{1W} = -\int_\infty^{\zeta_W}\left(\frac{\partial W_{0W}}{\partial z} - iU_{0W}\right)d\zeta_W = -\left[\frac{\partial^2\phi_0}{\partial z^2}-\phi_0\right]_{y=b}\int_\infty^{\zeta_W}\Gamma(\zeta_W)\,d\zeta_W = 0 \quad (4.18)$$

and the bracket before the second integral is essentially the Laplacian of the two-dimensional potential solution and hence vanishes. Consequently, there is no net exchange of pressure working between the inviscid interior and the side-wall through $\tilde{S}_W$. Detailed analysis of energy balance at $O(\epsilon)$ shows that the viscous dissipation within is exactly compensated from above by the pressure working at the strip of surface S_{MW}, which of course is supplied by the waves through the meniscus boundary layer $\tilde{S}_M$.

We record here that, if σ is taken as real, the wavenumber, according to (2.27), is given by

$$k = k_0 + \epsilon k_1, \quad (4.19a)$$

$$k_0 \tanh k_0 h = 1, \quad (4.19b)$$

$$k_1 = \frac{1-i}{\sqrt{2}}\frac{k_0}{b}\left(\frac{2k_0 b + \sinh 2k_0 h}{2k_0 h + \sinh 2k_0 h}\right). \quad (4.19c)$$

The imaginary part of k_1 agrees with the attenuation rate of Hunt (1952).

5. Concluding remarks

The discussion in §3 reveals that pressure working by the main core of the fluid gives energy to the meniscus boundary layer. Owing to the small volume, dissipation in the meniscus is negligible and the same energy is transmitted to the side-wall boundary layer underneath, also by pressure working. The role of viscosity in the meniscus layer is to make net pressure working possible, i.e. $\overline{p_d u_i n_i} \neq 0$. It is possible in certain examples (standing wave, §4) that the energy input from above cannot be totally dissipated in the side-wall boundary layer and the excess must be returned to the inviscid core through the side $\tilde{S}_W$ by pressure working. In the example of plane progressive waves in a rectangular channel, the excess is zero. Thus the meniscus plays an important role of an intermediary, although its internal dynamics is difficult to analyse in detail. This role is certainly not evident in the usual reckoning of viscous dissipation.

We have also found it necessary to exercise care in applying the boundary-layer–Poincaré method. In particular the second-order boundary-value problem for the potential involves a singular boundary condition at the rim of the free surface. Similar subtleties are likely to appear in interfacial wave problems if the complex frequency shift (not just its imaginary part) is desired.

Finally, we realize that our picture of energy transfer may appear peculiar to some readers' intuition. Indeed one of the referees believes that the energy transport vector should point from the interior of the fluid towards the side walls. Detailed measurement of the flow field would be needed to settle this issue.

Referees of an earlier version have been most helpful in their criticisms. Professor G. K. Batchelor's incisive comments led us finally to the right path. To all of them the authors are grateful. This work was begun under the sponsorship of National Science Foundation and the Coastal Engineering Research Center, U.S. Army, and the last revision was carried out while one of us (C. C. M.) was a visitor at the Department of Applied Mathematics and Theoretical Physics, University of Cambridge. The visit was made possible by the support of a Guggenheim Fellowship.

REFERENCES

Case, K. M. & Parkinson, W. C. 1957 Damping of surface waves in an incompressible liquid. *J. Fluid Mech.* **2**, 172.

Chu, V. H. & Mei, C. C. 1971 The nonlinear evoluation of Stokes waves on deep water. *J. Fluid Mech.* **47**, 337.

Dore, B. D. 1968 Viscous damping effects on long waves on the rotating earth. *Quart. J. Mech. Appl. Math.* **21**, 105–114.

Greenspan, H. P. 1968 *The Theory of Rotating Fluids*. Cambridge University Press.

Hunt, J. N. 1952 Viscous damping of waves over an inclined bed in a channel of finite width. *Houille Blanche*, **6**, 836.

Hunt, J. N. 1964 The viscous damping of gravity waves in shallow water. *Houille Blanche*, **6**, 685.

Johns, B. 1968 A boundary-layer method for the determination of the viscous damping of small amplitude gravity waves. *Quart. J. Mech. Appl. Math.* **21**, 93.

KEULEGAN, G. H. 1959 Energy dissipation in standing waves in rectangular basins. *J. Fluid Mech.* **6**, 33.

LANDAU, L. D. & LIFSHITZ, E. M. 1959 *Fluid Mechanics*. Pergamon.

LONGUET-HIGGINS, M. S. 1951 Ph.D. dissertation, University of Cambridge.

MILES, J. W. 1967 Surface wave damping in closed basins. *Proc. Roy. Soc.* A **297**, 459.

ÜNLÜATA, U. & MEI, C. C. 1970 Mass transport in water waves. *J. Geophys. Res.* **75**, 7611.

URSELL, F. 1952 Edge waves on a sloping beach. *Proc. Roy. Soc.* A **214**, 79.

WEHAUSEN, J. & LAITONE, E. 1960 Surface waves. *Handbuch der Physik*, vol. IX-3. Springer.